

## Heliospheric modulation of cosmic rays: Monthly reconstruction for 1951–2004

Ilya G. Usoskin,<sup>1</sup> Katja Alanko-Huotari,<sup>2</sup> Gennady A. Kovaltsov,<sup>3</sup> and Kalevi Mursula<sup>2</sup>

Received 2 June 2005; revised 14 October 2005; accepted 19 October 2005; published 23 December 2005.

[1] The differential energy spectrum of galactic cosmic rays in the vicinity of the Earth can be parameterized by the so-called force field model which has only one parameter, the modulation potential  $\phi$ , for a given local interstellar spectrum. Here we present the series of monthly values of the modulation potential  $\phi$  since February 1951, reconstructed using the data from the worldwide neutron monitor network and calibrated with precise balloon and space-borne direct measurements of cosmic ray energy spectrum. This work provides a long series of a parameter allowing for a quantitative estimate of the average monthly differential energy spectrum of cosmic rays near the Earth. A comparison with other occasional direct measurements of cosmic ray spectra confirms the reliability of the present reconstruction. The results can be applied in studies of long-term solar-terrestrial relations and the global evolution of the heliosphere.

**Citation:** Usoskin, I. G., K. Alanko-Huotari, G. A. Kovaltsov, and K. Mursula (2005), Heliospheric modulation of cosmic rays: Monthly reconstruction for 1951–2004, *J. Geophys. Res.*, 110, A12108, doi:10.1029/2005JA011250.

### 1. Introduction

[2] Energetic particles permanently bombard the Earth and form an important factor of solar-terrestrial relations. Cosmic ray flux has been monitored by ground-based neutron monitors for decades. At very long timescales it can be studied, e.g., by cosmogenic isotopes [see, e.g., Masarik and Beer, 1999; Usoskin *et al.*, 2003; McCracken *et al.*, 2004a; Solanki *et al.*, 2004]. However, all these data give an energy integrated flux, while the energy spectra of cosmic rays are directly available only for occasional balloon- or space-borne measurements during the last few decades and mostly for low energies. It is customary to use count rates of neutron monitors (or the cosmogenic isotope data) as a direct index of cosmic ray flux, but this is not exactly correct because different detectors are sensitive to different energies of cosmic rays [Alanko *et al.*, 2003].

[3] For many purposes it is important to know the differential energy spectrum of cosmic rays and its temporal variations. For example, the direct use of a linear relation between the energy-integrated cosmic ray flux and solar activity may lead to large uncertainties in long-term studies (see details in the work of Mursula *et al.* [2003] and Usoskin and Kovaltsov [2004]). Although it is hardly possible to reconstruct the past cosmic ray spectrum directly, the shape of the cosmic ray spectrum in the vicinity of the Earth can be well approximated by the so-called force field model [Gleeson and Axford, 1968; Caballero-Lopez and Moraal, 2004], which contains only one formal parameter,

the modulation potential. Attempts were made to reconstruct the series of the modulation potential in the past which, in the framework of the used model, allowed to estimate the energy spectrum [see, e.g., O'Brien and Burke, 1973; Chen *et al.*, 1994; Masarik and Beer, 1999; Usoskin *et al.*, 2002a]. Most of these results were based on different heliospheric modulation models and different data sets and therefore are not easy to compare with each other (see Appendix A). This has led to some confusion in the literature.

[4] Here we perform a detailed reconstruction of the monthly value of the modulation potential using all available data of the worldwide neutron monitor network since 1951. We also use occasional high-precision balloon and space-borne measurements to calibrate our model and make a link between fragmentary direct and continuous energy-integrated measurements of cosmic rays. We discuss random and systematic model-dependent uncertainties and compare the results with other estimates. The final series for the modulation parameter allows to evaluate the differential energy spectrum of galactic cosmic rays at the Earth for each month since February 1951. The paper is organized as follows. In section 2 we discuss the heliospheric modulation of cosmic rays, while section 3 deals with the details of neutron monitor measurements. Data selection and the analysis method are described in section 4, and the results are presented in section 5. In section 6 we give our conclusions. Appendix A is devoted to a comparison with other models.

### 2. Cosmic Rays Modulation Spectra

[5] Galactic cosmic rays (GCR) entering the heliosphere are affected by the interplanetary magnetic field and solar wind. This results in the modulation of their total flux and differential energy spectrum as measured in the vicinity of

<sup>1</sup>Sodankylä Geophysical Observatory (Oulu Unit), University of Oulu, Oulu, Finland.

<sup>2</sup>Department of Physical Sciences, University of Oulu, Oulu, Finland.

<sup>3</sup>Toffe Physical-Technical Institute, St. Petersburg, Russia.

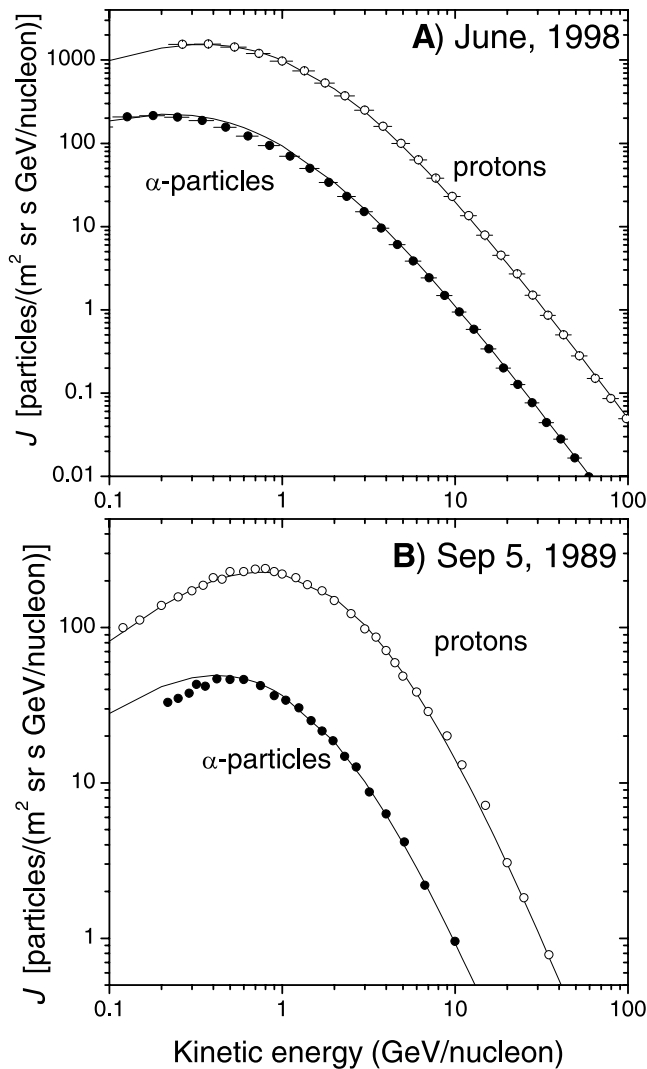


**Figure 1.** Differential energy spectra of cosmic rays. Open and filled circles depict the results of measurements for protons and  $\alpha$ -particles, respectively. Curves are the best fit model results. (a) Measurements by AMS-01 in June 1998 [Alcaraz *et al.*, 2000a, 2000b] fitted with  $\phi = 530 \pm 15$  MV. (b) Measurements by NMSU on 5 September 1989 [Webber *et al.*, 1991] fitted with  $\phi = 1350 \pm 25$  MV.

the Earth. The modulation varies with the varying solar activity and is often described in terms of the so-called force field model [Gleeson and Axford, 1968; Caballero-Lopez and Moraal, 2004; McCracken *et al.*, 2004a]. The only explicit parameter of this model is the modulation potential  $\phi$  whose value is given in units of MV. (In the literature it is also called the “force field parameter” and the “modulation strength.”) The value of  $Ze\phi$  corresponds to the average energy loss of cosmic rays inside the heliosphere. The theoretical basis for the force field approximation is quite limited due to a number of simplifying assumptions, such as spherically symmetric and steady-state heliosphere, negligible streaming of cosmic rays, and the diffusion coefficient with separable effects of heliodistance and energy/rigidity. For a detailed discussion see, e.g., Gleeson and Axford [1968] and McCracken *et al.* [2004a]. These conditions are often violated, in particular on short timescales and during

periods of high solar activity, which does not allow a direct application of the force field method to study the heliospheric transport of cosmic rays. However, despite its limited theoretical application, the force field model provides a useful way to parameterize the shape of GCR differential energy spectrum. Here we use it only in this sense. In fact, the model allows for a good fitting of the measured spectra.

[6] The differential intensity  $J_i$  of cosmic ray nuclei of type  $i$  at 1 AU is given as

$$J_i(T, \phi) = J_{\text{LIS},i}(T + \Phi) \frac{(T)(T + 2T_r)}{(T + \Phi)(T + \Phi + 2T_r)}, \quad (1)$$

where  $T$  is the kinetic energy (in MeV per nucleon) of cosmic nuclei with charge number  $Z$  and mass number  $A$  and  $\Phi = (Ze/A)\phi$ . The proton’s rest mass energy is  $T_r = 938$  MeV.  $J_{\text{LIS},i}$  denotes the local interstellar spectrum (LIS) of cosmic ray nuclei of type  $i$ .

[7] We stress that this approach not only contains the explicit modulation potential  $\phi$  which is often discussed but is also implicitly dependent on the fixed shape of the LIS. Here we use the LIS for protons according to [Burger *et al.*, 2000]

$$J_{\text{LIS}}(T) = \frac{1.9 \cdot 10^4 \cdot P(T)^{-2.78}}{1 + 0.4866 P(T)^{-2.51}}, \quad (2)$$

where  $P(T) = \sqrt{T(T + 2T_r)}$ .  $J$  and  $T$  are expressed in units of [particles/(m<sup>2</sup> sr s GeV/nucleon)] and in [GeV/nucleon], respectively. This equation corresponds to equation (2) in the work of Burger *et al.* [2000] within 2% accuracy but is easier to use and corrects a typographical error in the latter ( $P$  should read instead of  $P$  on the second line there (R. A. Burger and M. S. Potgieter, personal communication, 2002)). In Appendix A we discuss some other LIS approximations used in literature and compare the present results with those derived from other LIS approximations.

[8] An example of the fitting proton and  $\alpha$ -particle data with the force field model is shown in Figure 1. We choose two direct measurements of cosmic ray spectra performed in quite different heliospheric conditions. One is the precise measurement by AMS-01 carried out during a quiet solar period of 3–12 June 1998 [Alcaraz *et al.*, 2000a, 2000b]. Measured spectra were well fitted by the force field model with the modulation parameter  $\phi = 530 \pm 15$  MV (90% confidence interval). The other reference spectrum was measured during the NMSU balloon flight performed on 5 September 1989 [Webber *et al.*, 1991] during high solar activity. Note that the severe solar proton events of September–October 1989 came 3 weeks later. These data are well fitted by the force field model with the value of  $\phi = 1350 \pm 25$  MV (90% confidence interval). Other direct measurements of cosmic ray energy spectra can be fitted by the force field model equally well.

[9] According to recent precise measurements of GCR spectra and composition by, e.g., AMS, BESS, and CAPRICE experiments,  $\alpha$ -particles compose  $5\% \pm 0.2\%$  (in particle number) of GCR in the high energy range (above 10 GeV/nucleon). This ratio is constant, implying the similarity in their energy (per nucleon) spectra (see Figure 2). Therefore we use the number ratio  $\alpha/p = 0.05$  in LIS. Note that according to equation (1)  $\alpha$ -particles are less

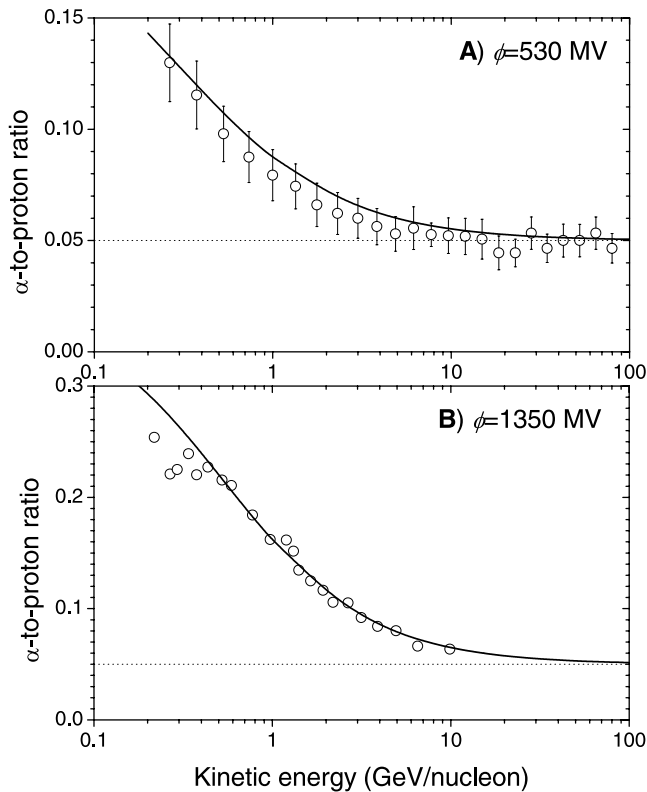


**Figure 2.** The  $\alpha$ -particle to proton number ratio at the Earth's orbit according to direct measurements (dots) and model calculations (solid line). The dotted line depicts the ratio (0.05) in the local interstellar space. (a) Measurements by AMS-01 in June 1998 [Alcaraz *et al.*, 2000a, 2000b] and model ratio with  $\phi = 530$  MV (cf. Figure 1a). (b) Measurements on 5 September 1989 [Webber *et al.*, 1991] and model ratio with  $\phi = 1350$  MV (cf. Figure 1b).

effectively influenced than protons by the heliospheric modulation process because of their smaller  $Z/A$  ratio. Correspondingly, the  $\alpha/p$ -ratio should increase with decreasing energy per nucleon, exactly as observed in direct measurements (Figure 2).

[10] Thus we conclude that the force field model provides a very useful and simple parametric approximation of the differential spectrum of galactic cosmic rays. This model contains only one variable parameter and, therefore, the whole energy spectrum (in the energy range from 100 MeV/nucleon to 100 GeV/nucleon) for protons and  $\alpha$ -particles can be described by a single number, the modulation potential  $\phi$ , within the framework of the adopted LIS. However, we warn again that  $\phi$  is only a formal spectral index whose physical interpretation is not straightforward, especially on short time scales and during periods of active Sun.

### 3. Neutron Monitor Count Rate

[11] A neutron monitor (NM) is an energy integrating cosmic ray detector whose total count rate can be presented as a sum of count rates  $N_i$  due to different species of GCR:

$$N = \sum_i N_i = \sum_i \int_{T_{ci}}^{\infty} J_i(T, \phi) Y_i(T) dT, \quad (3)$$

where  $Y_i$  is the specific yield function of NM for the  $i$ th species of GCR, and the integration is over kinetic energy above  $T_{ci}$ , which is the kinetic energy corresponding to the local geomagnetic rigidity cutoff  $P_c$  and is different for different species of cosmic rays. Here we only consider the two most abundant CR species, protons and  $\alpha$ -particles. Since the contribution of heavier species is small and their modulation is similar to that of helium, we did not consider them here. While the fraction of  $\alpha$ -particles is about 20% (in nucleon number) in LIS, their contribution to the NM count rate varies from 23% (polar NM, solar minimum) to 37% (equatorial NM, solar maximum).

[12] Here we consider two NM specific yield functions as shown in Figure 3 for a standard sea-level 1NM64 neutron monitor. All yield functions are computed for the sea level. One yield function is given by Clem and Dorman [2000] both for protons and  ${}^4\text{He}$ , leading to quite close curves (Figure 3). Since the other yield function by Debrunner *et al.* [1982] was calculated only for protons, we considered an  $\alpha$ -particle as four equal nucleons with the same energy per nucleon, i.e.,  $Y_\alpha = 4Y_p$ , in this case.

[13] The NM yield function is evaluated only up to the energy of 100 GeV/nucleon. However, as discussed below, more energetic cosmic rays also contribute significantly to NM count rate. This is taken into account in the following way. First, we have computed, applying equation (3) to protons and  $\alpha$ -particles with energy up to 100 GeV/nucleon, the expected count rate  $N_{st}$  of the standard NM (1NM64, sea level) for different values of the modulation parameter and the geomagnetic rigidity cutoff (Figure 4). Next, we notice that the modulation of GCR with energy of 100 GeV/nucleon is only about 1%, which can be neglected when comparing to tens of % in the GeV/nucleon energy range. Therefore we have assumed that the flux of GCR above 100 GeV/nucleon is constant in time. Then the expression for NM count rate is rewritten in the following form

$$N(\phi, P_c) = N_{st}(\phi, P_c) + N_0, \quad (4)$$

where  $N_0$  represents the portion of NM count rate due to GCR with energy above 100 GeV/nucleon and is assumed to be constant over the solar cycle. Because of the high energy of cosmic rays contributing to  $N_0$ , it is not affected

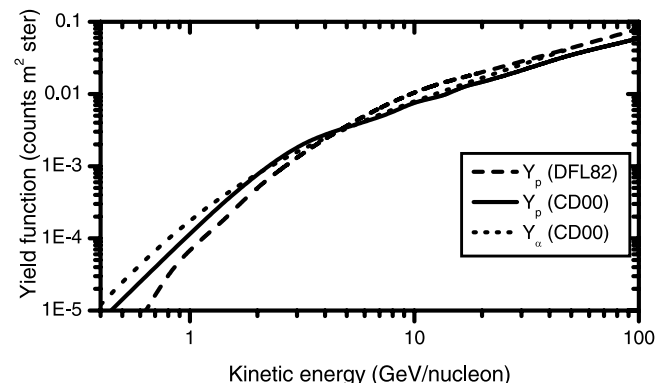


**Figure 3.** Specific yield function (per nucleon) of a standard sea-level 1-NM64 neutron monitor for protons  $Y_p$  and  $\alpha$ -particles  $Y_\alpha$  according to Debrunner *et al.* [1982] (DFL82) and Clem and Dorman [2000] (CD00).

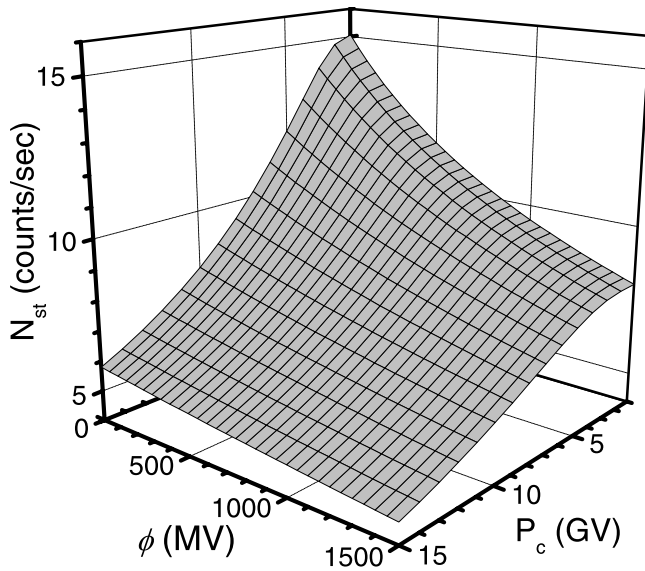


**Figure 4.** Standard neutron monitor count rate,  $N_{st}(\phi, P_c)$ , as a function of the modulation potential  $\phi$  and geomagnetic rigidity cutoff  $P_c$ . Both protons and  $\alpha$ -particles are included.

by the geomagnetic cutoff and is therefore the same for all NM stations. The exact value of  $N_o$  is an unknown parameter which should be fitted from the data.

## 4. Data and Analysis Method

### 4.1. Data Selection

[14] Although NM is an energy-integrating device, it allows for an estimate of GCR spectrum using the relation shown in Figure 4 and equation (4). Ideally, from the observed count rate of a NM with a given geomagnetic cutoff, one can evaluate the modulation potential  $\phi$ . However, the calculated expected count rate of the standard NM may not exactly correspond to the count rate of a real instrument. The reason is that each individual NM may differ in technical characteristics and environment (e.g., the building constructions, relative geometry, dead-time and high voltage setups, efficiency of registration, etc.) from the standard NM. Accordingly, each NM should be normalized to the standard conditions, assuming that its actual count rate is directly proportional to the expected count rate of the standard NM as described above. We also note a recent initiative by the North-West University (South Africa) on a direct intercalibration of different NM efficiency by means of a movable neutron monitor [Krüger *et al.*, 2003].

[15] Therefore two unknowns enter the procedure of  $\phi$  reconstruction from NM data: the contribution from high-energy cosmic rays  $N_o$  to the expected standard NM count rate (this unknown is the same for all NMs), and the scaling factor  $k$  normalizing the real NM observation conditions to the standard ones (this unknown is different for each NM). Thus the problem is now a typical ill-defined problem of fitting a model into data.

[16] In this study we have used all available NM data matching the following selection criteria: (1) neutron monitors should be of the same type and be located at a low altitude, in order to be close to the standard observational conditions; (2) neutron monitors should have operated

stably for a long period, with all changes in the efficiency, if any, properly recorded; (3) NM network should cover a range of geomagnetic cutoff rigidities. The list of NMs which match these criteria is given in the upper block of Table 1, together with their parameters and the period of stable operation. Before further analysis, the pressure corrected count rates of each NM were reduced to the standard observational conditions, i.e., divided by the number of NM64 counters and reduced to the sea-level pressure of 1000 mb using the individual barometric coefficients. Throughout the paper we use the momentary geomagnetic cutoff rigidity for each station which is an interpolation between 5-year epochs given by Shea and Smart [2001].

[17] For this study we also need reference periods when the value of  $\phi$  is measured independently and directly. We have chosen two reference periods which correspond to the precise measurements of GCR spectra and therefore allow to evaluate the modulation potential  $\phi$  directly. These periods also correspond to quite different heliospheric conditions. One is the period of 3–12 June 1998, with  $\phi_1 = 530 \pm 15$  MV, and the other is 5 September 1989, with  $\phi_2 = 1350 \pm 25$  MV (see Figure 1 and section 2). These two periods are used to normalize the NM count rates and to fix the unknown parameters.

### 4.2. Normalization of Neutron Monitor Count Rates

[18] For the two reference periods when the value of  $\phi$  is known independently, we can evaluate the unknown parameters in the following way. For two given values of  $\phi_1$  and  $\phi_2$  one can calculate the corresponding values of the variable part of the expected NM count rate  $N_{st,1}$  and  $N_{st,2}$  (see Figure 4). Then the expected total count rates of  $j$ th real NM can be written for these two periods as

$$C_{1j} = k_j(N_{st,1} + N_o), \quad C_{2j} = k_j(N_{st,2} + N_o). \quad (5)$$

These expected count rates  $C_{1j}$  and  $C_{2j}$  can then be compared with the actually observed count rates  $A_{1j}$  and  $A_{2j}$  during the corresponding reference periods. This provides  $2n$  equations with  $(n + 1)$  unknowns ( $n$  is the number of NMs in the study). The best-fit parameters were found by the least square technique. We define the discrepancy to be minimized as follows:

$$\epsilon = \sum_{j=1}^n (\ln^2(C_{1j}/A_{1j}) + \ln^2(C_{2j}/A_{2j})). \quad (6)$$

The log-discrepancy is chosen in order to give equal weights to the two reference periods. Otherwise we would

**Table 1.** List of Neutron Monitors Used in This Study and Their Characteristics: Altitude, m, Geomagnetic Rigidity Cutoff  $P_c$  (GV) for the 1995 Epoch and the Period of Data Used Here

| Name           | Type | Altitude | $P_c$ | Period          |
|----------------|------|----------|-------|-----------------|
| Goose Bay      | NM64 | 46       | 0.74  | 01/1965–12/1998 |
| Oulu           | NM64 | 15       | 0.77  | 04/1964–12/2004 |
| Kerguelen      | NM64 | 33       | 1.15  | 04/1964–12/2004 |
| Kiel           | NM64 | 54       | 2.4   | 01/1965–12/2003 |
| Hermanus       | NM64 | 26       | 4.5   | 01/1973–10/2002 |
| Rome           | NM64 | 60       | 6.3   | 01/1967–12/2004 |
| Climax         | IGY  | 3400     | 3     | 02/1951–12/2004 |
| Mt. Washington | IGY  | 1900     | 1.3   | 11/1955–06/1991 |

**Table 2.** Best-Fit Model Parameters for the Two NM Yield Functions by *Debrunner et al.* [1982] (DFL82) and by *Clem and Dorman* [2000] (CD00)

| Name             | $k_j$ (DFL82) | $k_j$ (CD00) |
|------------------|---------------|--------------|
| Goose Bay        | 1.03          | 1.02         |
| Hermanus         | 1.02          | 1.03         |
| Kerguelen        | 1.05          | 1.04         |
| Kiel             | 0.87          | 0.87         |
| Oulu             | 1.01          | 1.00         |
| Rome             | 0.95          | 0.97         |
| $N_o$ , counts/s | 5.33          | 5.88         |

overemphasize the reference period 1 (June 1998) where count rates were higher. The obtained best-fit parameters are listed in Table 2. An example of  $\epsilon$  as a function of  $N_o$  (all other parameters  $k_j$  being fixed) is shown in Figure 5.

[19] From Table 2 one can see that the efficiency of NM is close to the theoretically expected value (the scaling factors  $k$  close to unity), except for Kiel NM whose efficiency is somewhat above the standard expectation. It is important to note that the contribution of the very energetic cosmic rays is quite significant ( $N_o = 5.3\text{--}5.9$  counts/s) compared to the variable count rate  $N_{st}$  (Figure 4). It contributes from 1/4 (polar NM, solar minimum) to about a half (equatorial NM, solar maximum) of the total NM count rate. Accordingly, the contribution from the very high energy GCR provides a constant offset in the NM count rate.

## 5. Reconstruction of the Modulation Potential

### 5.1. Period After 1964

[20] We can now reconstruct the modulation potential  $\phi$  from NM count rates for the period after 1964 when a number of similar NMs of the NM64 type were launched. Using the fixed best-fit values of the scaling coefficients  $k_j$  (Table 2), the actual NM count rate is first scaled to the standard conditions. Then the value of  $N_o$  is subtracted, and finally, the estimate of  $\phi_j$  for  $j$ th NM is obtained from Figure 4 for the momentary geomagnetic rigidity cutoff. From a set of  $\phi_j$  we compute, using all available NMs at any time, the mean value  $\phi$  and its standard deviation  $\sigma$  which serves as the error of  $\phi$  reconstruction.

[21] We calculated the mean  $\phi$  separately for the two yield functions by *Debrunner et al.* [1982] and *Clem and*

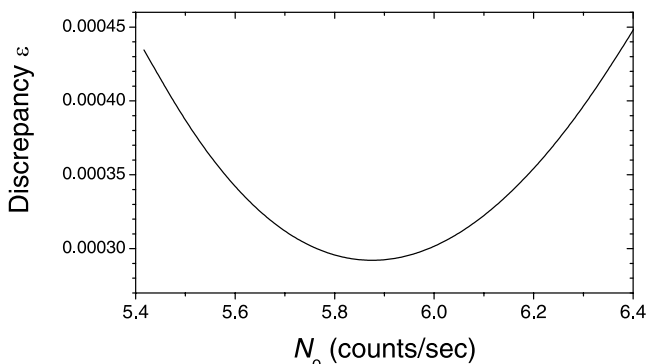


**Figure 5.** The discrepancy  $\epsilon$  (equation (6)) as a function of the parameter  $N_o$  (other parameters  $k_j$  being fixed at their best-fit values), using the CD00 yield function.

*Dorman* [2000], denoting the corresponding values by indices “DFL82” and “CD00.” While the two sets of  $\phi$  lie very close to each other (cross-correlation coefficient is better than 0.999), the difference  $\Delta\phi = \phi_{CD00} - \phi_{DFL82}$  is systematic and tends to cluster around a nearly parabolic shape (see Figure 6). Some excursions from this parabolic concentration are related either to strong solar proton events or to large Forbush decreases. The best parabolic fit (see Figure 6) gives an estimate of the systematic uncertainty so that  $\delta\phi = 0.5\langle|\Delta\phi|\rangle$ .

[22] As the final modulation parameter we take the mean of the two above  $\phi$  values, with the final uncertainty being a superposition of the random errors  $\sigma$  and the systematic uncertainty  $\delta\phi$ :

$$\phi = (\phi_{DFL82} + \phi_{CD00})/2$$

$$\sigma_\phi = \delta\phi + \sqrt{\frac{\sigma_{DFL82}^2 + \sigma_{CD00}^2}{n-1}}, \quad (7)$$

where  $n$  is the number of NMs whose data are available at the given month. The mean value of  $\sigma_\phi$  is 37 MV. The maximum deviation  $\sigma_\phi = 148$  MV in June 1991 is mainly due to the systematic uncertainty. Therefore we can conclude that the value of  $\phi$  is reconstructed within the accuracy of 50 MV (90% confidence level) after 1964. The reconstructed monthly values of  $\phi$  are shown in Figure 7.

[23] Large uncertainties in the value  $\phi$  appear during Forbush decreases when the CR spectrum is distorted. A Forbush decrease is caused by an interplanetary shock passing by the Earth, and it only weakly depends on the particle’s energy. Actually, lower energies can be even populated by locally accelerated particles. Therefore the CR spectrum during a Forbush decrease cannot be described by the same shape (force field formula) as the “normally” modulated spectrum, and the value of  $\phi$  becomes uncertain.

### 5.2. Period Before 1964

[24] It is difficult to apply the above-described method for the period before 1964, when only a few neutron monitors of IGY type, located at high altitudes, were available. Still, we have used two IGY-type NMs, Climax and Mt. Wash-

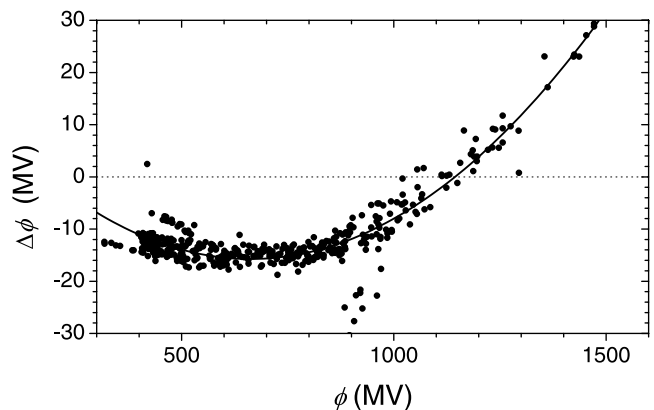


**Figure 6.** The difference between the monthly values of  $\phi$  reconstructed for 1964–2003, using the two different yield functions. The line is a parabolic fit, which gives an estimate of a systematic uncertainty of the model.

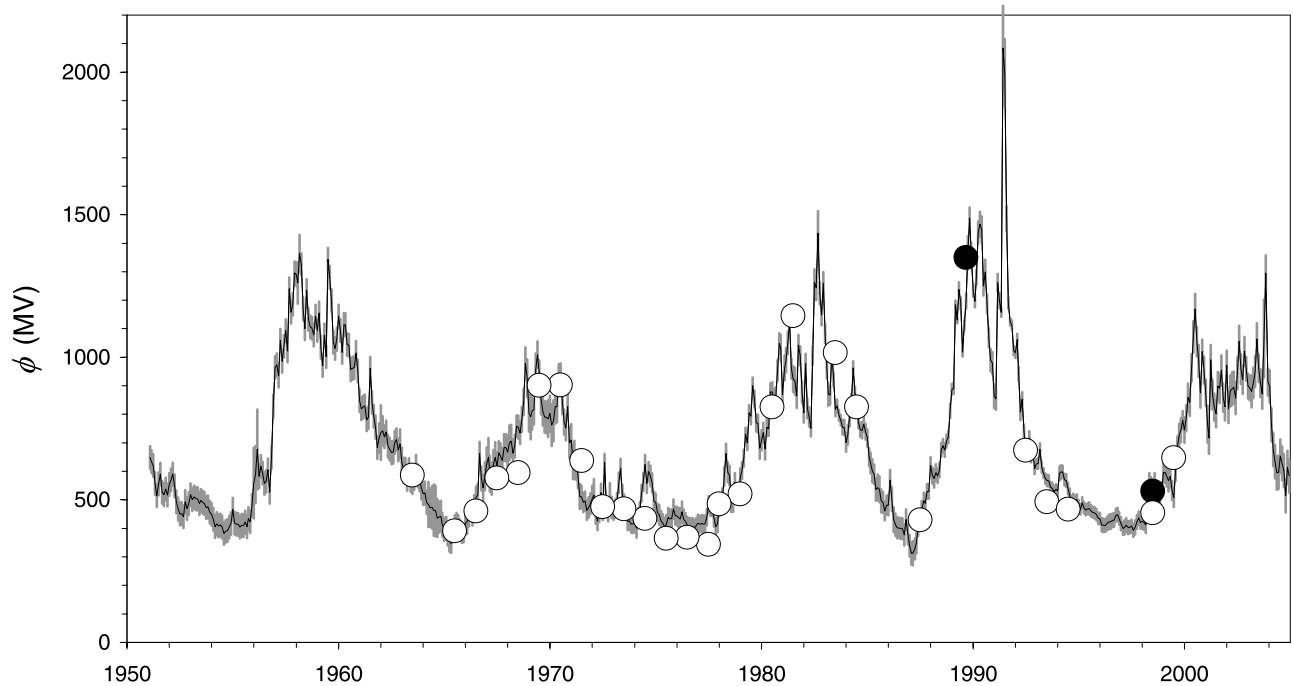


**Figure 7.** The reconstructed modulation parameter  $\phi$  (solid line) together with 68% confidence intervals (grey shading). Two large black dots denote the reference periods (see text). Open dots correspond to some fragmentary estimates of the cosmic ray spectrum from balloon or space-borne experiments. Limitations of the interpretation of the value of  $\phi$  are discussed in section 6.

ington (see Table 1), that have been in operation since 1950s. We did not include Huancayo NM (IGY, 3400 m altitude) since its record is quite noisy because of the low count rate due to equatorial location ( $P_c \approx 13$  GV). We note that only one yield function estimate is available for IGY-type NMs [Clem and Dorman, 2000]. This yield function was computed for the sea-level. However, a simple barometric correction for the high-latitude location leads to large uncertainties. Therefore we include this unknown uncertainty in the coefficients  $k$  and  $N_o$  of equation (5) which are calculated independently for IGY-type NMs using the period of overlapping observations with NM64-type NMs (i.e., after 1964). The best-fit coefficients (reduced to the sea-level NM64) were found to be  $k = 1.13$  (0.34) and  $N_o = 5.89$  counts/s (9.1 counts/s) for Climax (resp., Mt. Washington). The cross-correlation between the values of  $\phi$  obtained from NM64 (section 5.1) and IGY-type NM data, during the period after 1964 is 0.997 (see Figure 8). Using these coefficients and monthly data of Climax NM (since 1953 and, with some caveats, since February 1951) and Mt. Washington NM (since November 1955), we have calculated the value of the modulation parameter for the period 1951–1963. Errors were estimated similarly as in section 5.1.

### 5.3. Final Results

[25] The combined reconstruction of  $\phi$  is shown in Figure 7 and given in Table 3. The 68% confidence intervals are shown as grey shading and are typically below 40 MV after 1973 and below 60 MV before that. The mean 68% confidence level uncertainty is 38.5 MV. We note that the uncertainties (random part) are almost independent of the value of  $\phi$  and their small value (5–10%) confirms the validity of the used here parameterization of the GCR

spectral shape. During three severe events (Forbush decreases or GLE) the uncertainty increased up to 140 MV (in March 1956, June 1991, and October 2003) because of the distortion of the cosmic ray energy spectrum.

[26] In order to check the consistency of the reconstruction, we have compared it with the values of  $\phi$  obtained from various occasional direct balloon and space-borne measurements of CR spectrum [see, e.g., Ormes and Webber, 1968; Hsieh et al., 1971; Garcia-Munoz et al.,

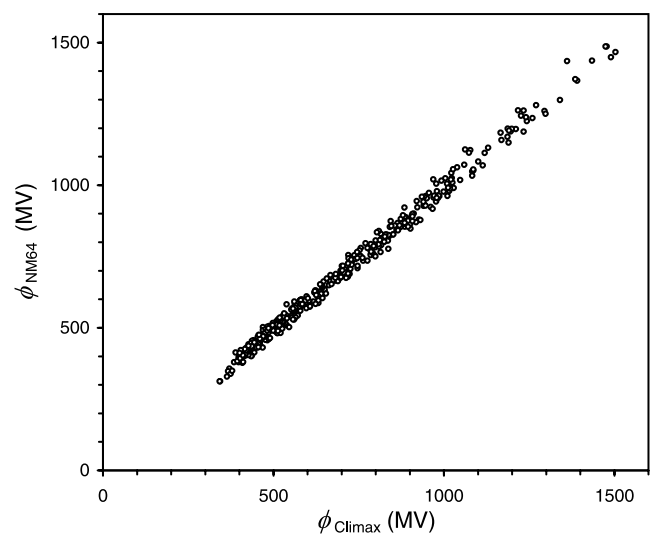


**Figure 8.** The scatter plot of the monthly values of  $\phi$  obtained from Climax IGY NM and standard NM64-type NM data for 1964–2003.

**Table 3.** Reconstructed Monthly Values of the Modulation Parameter  $\phi$ , MV<sup>a</sup>

| Year | Jan  | Feb  | Mar  | Apr  | May  | Jun  | Jul  | Aug  | Sep  | Oct  | Nov  | Dec  | Annual |
|------|------|------|------|------|------|------|------|------|------|------|------|------|--------|
| 1951 | –    | 649  | 633  | 620  | 558  | 514  | 556  | 590  | 526  | 518  | 538  | 516  | 567    |
| 1952 | 554  | 570  | 590  | 549  | 493  | 468  | 451  | 452  | 441  | 494  | 469  | 487  | 498    |
| 1953 | 518  | 501  | 510  | 504  | 503  | 486  | 498  | 492  | 487  | 473  | 476  | 457  | 489    |
| 1954 | 449  | 432  | 406  | 416  | 409  | 412  | 404  | 382  | 390  | 392  | 404  | 417  | 397    |
| 1955 | 467  | 418  | 415  | 414  | 405  | 411  | 410  | 422  | 405  | 434  | 423  | 480  | 415    |
| 1956 | 559  | 589  | 677  | 583  | 617  | 594  | 558  | 565  | 605  | 527  | 650  | 829  | 574    |
| 1957 | 964  | 973  | 934  | 1059 | 987  | 1039 | 1093 | 1022 | 1240 | 1158 | 1187 | 1296 | 1069   |
| 1958 | 1290 | 1261 | 1364 | 1326 | 1171 | 1101 | 1233 | 1133 | 1107 | 1102 | 1078 | 1144 | 1151   |
| 1959 | 1094 | 1155 | 1035 | 971  | 1077 | 1002 | 1343 | 1280 | 1199 | 1053 | 1031 | 1064 | 1090   |
| 1960 | 1143 | 1094 | 1017 | 1115 | 1114 | 1044 | 1043 | 957  | 962  | 964  | 1015 | 952  | 1033   |
| 1961 | 848  | 819  | 826  | 830  | 781  | 789  | 961  | 842  | 793  | 755  | 683  | 717  | 798    |
| 1962 | 736  | 741  | 721  | 738  | 688  | 678  | 666  | 667  | 702  | 711  | 674  | 696  | 692    |
| 1963 | 631  | 603  | 607  | 572  | 607  | 568  | 560  | 576  | 618  | 585  | 570  | 542  | 575    |
| 1964 | 522  | 525  | 491  | 483  | 472  | 474  | 464  | 462  | 436  | 440  | 442  | 413  | 460    |
| 1965 | 396  | 401  | 379  | 357  | 348  | 393  | 412  | 419  | 413  | 401  | 379  | 383  | 391    |
| 1966 | 418  | 425  | 446  | 457  | 436  | 482  | 509  | 517  | 662  | 574  | 542  | 583  | 503    |
| 1967 | 626  | 650  | 592  | 574  | 624  | 649  | 619  | 665  | 653  | 639  | 684  | 683  | 639    |
| 1968 | 667  | 700  | 706  | 663  | 688  | 758  | 755  | 735  | 782  | 843  | 979  | 927  | 764    |
| 1969 | 804  | 791  | 813  | 816  | 957  | 1009 | 942  | 854  | 812  | 791  | 789  | 784  | 846    |
| 1970 | 802  | 761  | 777  | 827  | 827  | 931  | 928  | 848  | 773  | 752  | 827  | 700  | 811    |
| 1971 | 710  | 634  | 640  | 618  | 587  | 512  | 511  | 491  | 495  | 464  | 473  | 486  | 550    |
| 1972 | 504  | 517  | 452  | 426  | 456  | 525  | 460  | 631  | 473  | 460  | 502  | 474  | 489    |
| 1973 | 460  | 470  | 494  | 559  | 610  | 519  | 488  | 463  | 425  | 425  | 414  | 416  | 478    |
| 1974 | 418  | 401  | 435  | 458  | 523  | 562  | 624  | 558  | 599  | 584  | 560  | 495  | 516    |
| 1975 | 490  | 456  | 447  | 426  | 418  | 405  | 415  | 439  | 433  | 435  | 468  | 445  | 440    |
| 1976 | 443  | 437  | 433  | 458  | 431  | 424  | 411  | 407  | 406  | 406  | 402  | 409  | 422    |
| 1977 | 419  | 415  | 417  | 414  | 415  | 439  | 483  | 473  | 472  | 436  | 406  | 416  | 434    |
| 1978 | 475  | 492  | 506  | 582  | 662  | 596  | 585  | 491  | 491  | 561  | 523  | 526  | 540    |
| 1979 | 578  | 603  | 646  | 731  | 700  | 806  | 793  | 900  | 853  | 770  | 767  | 681  | 732    |
| 1980 | 709  | 735  | 678  | 754  | 750  | 879  | 878  | 848  | 859  | 954  | 1048 | 1033 | 838    |
| 1981 | 870  | 962  | 990  | 1051 | 1123 | 961  | 924  | 917  | 864  | 1042 | 1005 | 879  | 964    |
| 1982 | 805  | 977  | 820  | 791  | 751  | 1005 | 1262 | 1243 | 1435 | 1224 | 1149 | 1260 | 1042   |
| 1983 | 1083 | 963  | 870  | 867  | 1025 | 922  | 819  | 829  | 796  | 780  | 755  | 754  | 868    |
| 1984 | 701  | 728  | 793  | 839  | 962  | 874  | 835  | 771  | 746  | 744  | 765  | 739  | 790    |
| 1985 | 717  | 649  | 629  | 602  | 590  | 536  | 543  | 537  | 496  | 491  | 461  | 481  | 556    |
| 1986 | 482  | 568  | 502  | 430  | 413  | 403  | 401  | 400  | 399  | 377  | 430  | 380  | 439    |
| 1987 | 339  | 312  | 312  | 329  | 349  | 404  | 432  | 464  | 497  | 488  | 529  | 529  | 420    |
| 1988 | 620  | 587  | 575  | 596  | 584  | 604  | 675  | 690  | 675  | 707  | 721  | 812  | 661    |
| 1989 | 887  | 892  | 1184 | 1131 | 1238 | 1189 | 1018 | 1113 | 1197 | 1366 | 1486 | 1371 | 1176   |
| 1990 | 1235 | 1197 | 1280 | 1437 | 1467 | 1448 | 1250 | 1298 | 1188 | 1069 | 990  | 980  | 1246   |
| 1991 | 864  | 854  | 1261 | 1198 | 1158 | 2084 | 1997 | 1486 | 1191 | 1125 | 1114 | 1024 | 1255   |
| 1992 | 1015 | 1063 | 942  | 808  | 853  | 742  | 675  | 688  | 717  | 652  | 672  | 610  | 791    |
| 1993 | 626  | 628  | 678  | 615  | 594  | 575  | 568  | 566  | 544  | 541  | 529  | 536  | 594    |
| 1994 | 531  | 592  | 597  | 598  | 571  | 568  | 540  | 515  | 494  | 504  | 495  | 501  | 550    |
| 1995 | 480  | 467  | 490  | 472  | 464  | 469  | 470  | 461  | 456  | 454  | 448  | 435  | 476    |
| 1996 | 434  | 412  | 411  | 409  | 417  | 422  | 423  | 427  | 430  | 446  | 449  | 435  | 440    |
| 1997 | 417  | 399  | 403  | 411  | 403  | 404  | 408  | 393  | 403  | 423  | 437  | 420  | 424    |
| 1998 | 425  | 421  | 412  | 509  | 567  | 550  | 510  | 564  | 511  | 475  | 498  | 536  | 510    |
| 1999 | 596  | 595  | 583  | 567  | 583  | 533  | 508  | 603  | 685  | 726  | 744  | 780  | 637    |
| 2000 | 745  | 787  | 859  | 841  | 963  | 1071 | 1170 | 1055 | 988  | 875  | 1019 | 955  | 957    |
| 2001 | 874  | 766  | 717  | 991  | 868  | 825  | 801  | 899  | 891  | 954  | 858  | 826  | 871    |
| 2002 | 973  | 819  | 881  | 889  | 894  | 857  | 944  | 1056 | 959  | 921  | 1020 | 959  | 954    |
| 2003 | 899  | 893  | 880  | 911  | 949  | 1065 | 961  | 910  | 872  | 959  | 1295 | 913  | 959    |
| 2004 | 898  | 764  | 677  | 633  | 595  | 596  | 653  | 628  | 602  | 514  | 614  | 584  | 647    |

<sup>a</sup>Limitations of the interpretation of the modulation potential are discussed in text. The last column presents the mean annual  $\phi$  (not the average of the monthly  $\phi$  values but calculated directly from annual NM data).

1975; *Mewaldt et al.*, 1976; *Kroeger*, 1986; *Seo et al.*, 1991; *McDonald et al.*, 1992; *Boenzio et al.*, 1999; *Sanuki et al.*, 2000; *Wang et al.*, 2002; *Asaoka et al.*, 2002; *Cane*, 2003, and references therein], shown as open dots in Figure 7. One can see that the reconstructed curve follows these dots quite reliably. Note that these data were not used in the reconstruction and therefore can serve as an independent test. The agreement is quite within 95% confidence ( $2\sigma$ ) level for all points. Keeping in mind that the balloon borne measurements are short-term (only several hours), a slight difference between them and the monthly averages is not

surprising. Although space-borne measurements are longer than balloon-based, they cover a smaller energy range and therefore generally yield a less precise estimate of  $\phi$ .

## 6. Conclusions

[27] We have presented the series of monthly values of the GCR modulation potential  $\phi$  since February 1951 (see Table 3 and Figure 7), reconstructed using the data from the worldwide neutron monitor network calibrated with direct balloon and space-borne measurements of cosmic

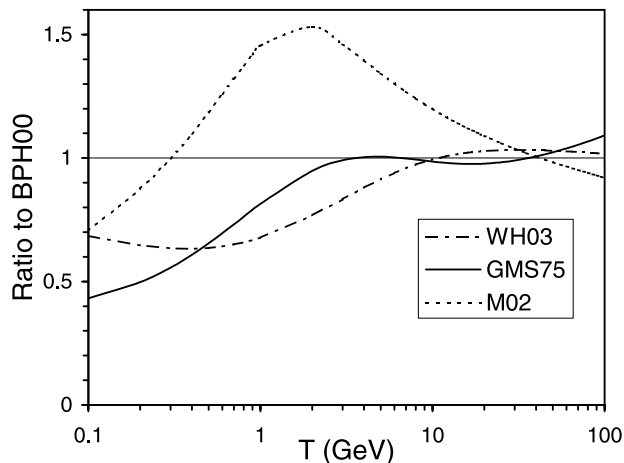


**Figure A1.** The ratio of different estimates of the local interstellar spectrum [Burger *et al.*, 2000, BPH00; Webber and Highbie, 2003, WH03; Garcia-Munoz *et al.*, 1975, GMS75; Moskalenko *et al.*, 2002, M02], divided by the BPH00.

ray spectra. This work provides a long series of a parameter allowing for a quantitative monthly estimate of the differential energy spectrum of cosmic rays near the Earth. The energy spectrum of cosmic rays is well parameterized by  $\phi$  and can be evaluated at any time from the average monthly value of  $\phi$  (Table 3) using equations (1) and (2). A comparison with occasional direct measurements of GCR spectra confirms the reliability of the present reconstruction.

[28] We note again that the modulation potential obtained here only serves as a formal parameter describing the shape of the GCR differential energy spectrum. It would be incorrect to use it as a proxy for momentary conditions in the heliosphere because of the limitations of the force field model (see McCracken *et al.* [2004a], Caballero-Lopez and Moraal [2004], and section 2). We also note that the force field approximation becomes invalid during periods of very strong interplanetary transient phenomena such as Forbush decreases.

[29] We have also found that high-energy (above 100 GeV/nucleon) cosmic rays contribute significantly to the neutron monitor count rate. This will require a detailed calculation of the specific yield function in the very high energy range, above the presently available energy range. The results of the present work can be applied in studies of long-term solar-terrestrial relations, such as, e.g., cosmogenic isotope production and atmospheric ionization [see, e.g., Jöckel and Brenninkmeijer, 2002; McCracken *et al.*, 2004b; Usoskin *et al.*, 2004a, 2004b].

## Appendix A: Comparison With Other Models

[30] While our method is based on the local interstellar spectrum by [Burger *et al.*, 2000] (called BPH00; see also equation (2)), some other estimates of LIS can be found in literature. Among the most commonly used LIS approxi-

mations is the one suggested by [Garcia-Munoz *et al.*, 1975]

$$J_{\text{LIS}}(T) = 9.9 \cdot 10^8 (T + 780 \exp(-0.00025 T))^{-2.65}, \quad (\text{A1})$$

where  $T$  and  $J$  are given in MeV and in [particles/(sr m<sup>2</sup> s MeV)], respectively. This LIS (called GMS75) underestimates the low energy part and overestimates the high-energy part of the spectrum because of the small spectral index  $-2.65$ , leading to somewhat worse fitting of the measured spectra than BPH00. Another LIS approximation was recently given by Webber and Highbie [2003] (WH03) as

$$J_{\text{LIS}}(T) = \frac{2.11 \cdot 10^4 \cdot T^{-2.80}}{1 + 5.85 T^{-1.22} + 1.18 T^{-2.54}}, \quad (\text{A2})$$

where  $T$  and  $J$  are given in GeV and in [particle/(sr m<sup>2</sup> s GeV)], respectively. Recently, Moskalenko *et al.* [2002] evaluated LIS, using a complex propagation model of particles in the galaxy and accounting for different species. This LIS for protons was parameterized by [Langner, 2004]

$$J_{\text{LIS}}(T) = \begin{cases} \exp(4.64 - 0.08(\ln T)^2 - 2.91\sqrt{T}), & \text{if } T < 1 \text{ GeV} \\ \exp(3.22 - 2.86(\ln T) - 1.50/T), & \text{if } T > 1 \text{ GeV} \end{cases} \quad (\text{A3})$$

These LIS estimates are compared in Figure A1 which shows the ratio of other spectra to BPH00. While in a relatively good agreement with each other above 10 GeV, the three models greatly differ (by a factor of 2) in low energy range. Since LIS is an important factor in the force field model (equation (1)), the exact relation between the value of  $\phi$  and the differential energy spectrum of GCR is model dependent. We have compared the results obtained using different LIS models and provide a method to recalculate them between each other.

[31] In particular, we would like to discuss the modulation model by Castagnoli and Lal [1980] which uses the GMS75 LIS and is widely used in applied studies. Note that the final formula [Castagnoli and Lal, 1980, equation (1)] contains an error (repeated in numerous later papers, e.g., Masarik and Beer [1999]) and does not represent the exact force field model. According to the exact force field model,  $(T + \Phi)$  should substitute the energy in the expression for LIS (see, e.g., Caballero-Lopez and Moraal [2004] and our equation (1)). In the formula by Castagnoli and Lal [1980]  $(T + \Phi)$  enters only in the first linear term of the expression for LIS but not in the exponential term (see equation (A1) above). Accordingly, this distorts the shape of the modeled GCR spectrum and provides a worse fit to observations. For example, the June 1998 proton spectrum measured by AMS (see Figure 1a) can be fitted with this model with the  $\chi^2$  statistics (with 23 degrees of freedom) being  $\chi^2(23) = 27$  while the used above model (equations (1) and (2)) provides a better fit  $\chi^2(23) = 7$ .

[32] Although these models are quite different from each other, all of them allow for a reasonable parameterization of the modulated GCR spectrum at 1 AU, only the exact



values of  $\phi$  are model-dependent. We have repeated the calculations for the four LIS and found that the relation between the different reconstructions of  $\phi$  closely follows a linear relation. The value of  $\phi_i$  obtained using the LIS approximation by *Webber and Higbie* [2003] (denoted as  $\phi_{WH03}$ ), by *Garcia-Munoz et al.* [1975] ( $\phi_{GMS75}$ ), by *Moskalenko et al.* [2002] ( $\phi_{M02}$ ) and from the models by *Castagnoli and Lal* [1980] ( $\phi_{CL80}$ ) are related to  $\phi_o$  obtained in this work (Table 3) as

$$\begin{aligned}\phi_{WH03} &= 0.97\phi_o - 110 \text{ MV}, \\ \phi_{GMS75} &= 1.04\phi_o - 76 \text{ MV}, \\ \phi_{CL80} &= 0.97\phi_o - 78 \text{ MV}, \\ \phi_{M02} &= 1.12\phi_o + 92 \text{ MV},\end{aligned}\tag{A4}$$

Using these relations one can convert the reconstructed values of the modulation parameter into those comparable with earlier estimates. However, such a conversion increases the uncertainties because the above formula is only an approximation. We note that there is a systematic offset between values of  $\phi$  obtained using “empirically” derived LIS and those using theoretically computed LIS, due to the excess of the latter [*Moskalenko et al.*, 2002] in the range of 1–10 GeV. The difference can be as large as several hundred MV. The reference LIS used here (BPH00) lies in between these two.

[33] We would also like to note that the present evaluation of the modulation potential is different from the  $\phi_{U02}$  evaluated earlier by *Usoskin et al.* [2002a, 2002b]. In the 2002 paper we considered only protons and neglected  $\alpha$ -particles, thus underestimating the values of  $\phi_{U02}$ , which is, however, still in a nearly linear relation with  $\phi_o$ :  $\phi_{U02} = 0.87\phi_o - 89 \text{ MV}$ .

[34] **Acknowledgments.** We acknowledge the support from the Academy of Finland, the Finnish Academy of Science and Letters (Vilho, Yrjö, and Kalle Väisälä Foundation), the Finnish graduate school in astronomy and space physics, and the Russian Academy of Sciences (Programme of Fundamental Research 30). NM data were received through the WDC-C2. National Science Foundation grant ATM-9912341 is acknowledged for Climax NM data. North-West University (Potchefstroom, South Africa) is acknowledged for the Hermanus NM data. IPEV, Brest, and Paris Observatory are thanked for the Kerguelen NM data. Christian-Albrechts University of Kiel is thanked for the Kiel NM data. Rome NM is supported by IFSI/INAF-UNIRoma3 collaboration. Data of Oulu NM are available at <http://cosmicrays oulu.fi>.

[35] Shadia Rifai Habbal thanks Jonathan F. Ormes and another referee for their assistance in evaluating this paper.

## References

Alanko, K., I. G. Usoskin, K. Mursula, and G. A. Kovaltsov (2003), Heliospheric modulation strength and the neutron monitor effective energy, *Adv. Space Res.*, **32**, 615.  
 Alcaraz, J., et al. (2000a), Cosmic protons, *Phys. Lett. B*, **490**, 27.  
 Alcaraz, J., et al. (2000b), Helium in near Earth orbit, *Phys. Lett. B*, **494**, 193.  
 Asaoka, Y., et al. (2002), Measurements of cosmic-ray low-energy antiproton and proton spectra in a transient period of solar field reversal, *Phys. Rev. Lett.*, **88**, 051101.  
 Boenzio, M., et al. (1999), The cosmic-ray proton and helium spectra between 0.4 and 200 GV, *Astrophys. J.*, **518**, 457.  
 Burger, R. A., M. S. Potgieter, and B. Heber (2000), Rigidity dependence of cosmic ray proton latitudinal gradients measured by the Ulysses spacecraft: Implication for the diffusion tensor, *J. Geophys. Res.*, **105**, 27,447.

Caballero-Lopez, R. A., and H. Moraal (2004), Limitations of the force field equation to describe cosmic ray modulation, *J. Geophys. Res.*, **109**, A01101, doi:10.1029/2003JA010098.  
 Cane, D. (2003), Influence of solar activity variations on the interplanetary space, Ph.D. thesis, 134 pp., Univ. of Torino, Torino, Italy.  
 Castagnoli, G., and D. Lal (1980), Solar modulation effects in terrestrial production of carbon-14, *Radiocarbon*, **22**, 133.  
 Clem, J. M., and L. I. Dorman (2000), Neutron monitor response functions, *Space Sci. Rev.*, **93**, 335.  
 Chen, J., et al. (1994), A model of galactic cosmic rays for use in calculating linear energy transfer spectra, *Adv. Space Res.*, **14**, (10)765.  
 Debrunner, H., E. Flueckiger, and J. A. Lockwood (1982), Specific yield function S(P) for a neutron monitor at sea level, paper presented at 8th European Cosmic Ray Symposium, Rome.  
 Garcia-Munoz, M., G. M. Mason, and J. A. Simpson (1975), The anomalous  $^4\text{He}$  component in the cosmic-ray spectrum at  $\leq 50$  MeV per nucleon during 1972–1974, *Astrophys. J.*, **202**, 265.  
 Gleeson, L. J., and W. I. Axford (1968), Solar modulation of galactic cosmic rays, *Astrophys. J.*, **154**, 1011.  
 Hsieh, K. C., G. M. Mason, and J. A. Simpson (1971), Cosmic-Ray  $^2\text{H}$  from satellite measurements, 1965–1969, *Astrophys. J.*, **166**, 221.  
 Jöckel, P., and C. A. M. Brenninkmeijer (2002), The seasonal cycle of cosmogenic  $^{14}\text{C}$  at the surface level: A solar cycle adjusted, zonal-average climatology based on observations, *J. Geophys. Res.*, **107**(D22), 4656, doi:10.1029/2001JD001104.  
 Kroeger, R. (1986), Measurements of hydrogen and helium isotopes in Galactic cosmic rays from 1978 through 1984, *Astrophys. J.*, **303**, 816.  
 Krüger, X., et al. (2003), First results of a mobile neutron monitor to intercalibrate the worldwide network, in *Proc. 28th Int. Cosmic Ray Conf.*, 3441.  
 Langner, U. (2004), Effects of termination shock acceleration on cosmic rays in the heliosphere, Ph.D. thesis, 162 pp., North-West University, Potchefstroom, South Africa.  
 Masarik, J., and J. Beer (1999), Simulation of particle fluxes and cosmogenic nuclide production in the Earth's atmosphere, *J. Geophys. Res.*, **104**, 12,099.  
 McCracken, K. G., F. B. McDonald, J. Beer, G. Raisbeck, and F. Yiou (2004a), A phenomenological study of the long-term cosmic ray modulation 850–1958 AD, *J. Geophys. Res.*, **109**, A12103, doi:10.1029/2004JA010685.  
 McCracken, K. G., J. Beer, and F. B. McDonald (2004b), Variations in the cosmic radiation, 1890–1986, and the solar and terrestrial implications, *Adv. Space Res.*, **34**, 397.  
 McDonald, F. B., et al. (1992), The cosmic radiation in the heliosphere at successive solar minima, *J. Geophys. Res.*, **97**, 1557.  
 Mewaldt, R. A., E. C. Stone, and R. E. Vogt (1976), The isotopic composition of hydrogen and helium in low-energy cosmic rays, *Astrophys. J.*, **206**, 616.  
 Moskalenko, I. V., A. W. Strong, J. F. Ormes, and M. S. Potgieter (2002), Secondary antiprotons and propagation of cosmic rays in the galaxy and heliosphere, *Astrophys. J.*, **565**, 280.  
 Mursula, K., I. G. Usoskin, and G. A. Kovaltsov (2003), Reconstructing the long-term cosmic ray intensity: Linear relations do not work, *Ann. Geophys.*, **21**, 863.  
 O'Brien, K., and G. P. Burke (1973), Calculated cosmic ray neutron monitor response to solar modulation of galactic cosmic rays, *J. Geophys. Res.*, **78**, 3013.  
 Ormes, J. F., and W. R. Webber (1968), Proton and helium nuclei cosmic ray spectra and modulations between 100 and 200 MeV/nucleon, *J. Geophys. Res.*, **73**, 4231.  
 Sanuki, T., et al. (2000), Precise measurement of cosmic-ray proton and helium spectra with the BESS spectrometer, *Astrophys. J.*, **545**, 1135.  
 Seo, E. S., et al. (1991), Measurement of cosmic-ray proton and helium spectra during the 1987 solar minimum, *Astrophys. J.*, **378**, 763.  
 Shea, M. A., and D. F. Smart (2001), Vertical cutoff rigidities for cosmic ray stations since 1955, *Proc. 27th Int. Cosmic Ray Conf.*, 4063.  
 Solanki, S. K., I. G. Usoskin, B. Kromer, M. Schüssler, and J. Beer (2004), An unusually active Sun during recent decades compared to the previous 11,000 years, *Nature*, **431**, 1084.  
 Usoskin, I. G., and G. A. Kovaltsov (2004), Long-term solar activity: Direct and indirect study, *Solar Phys.*, **224**, 37.  
 Usoskin, I. G., K. Alanko, K. Mursula, and G. A. Kovaltsov (2002a), Heliospheric modulation strength during the neutron monitor era, *Solar Phys.*, **207**, 389.  
 Usoskin, I. G., K. Mursula, S. Solanki, M. Schüssler, and G. A. Kovaltsov (2002b), Physical reconstruction of cosmic ray intensity since 1610, *J. Geophys. Res.*, **107**(A11), 1374, doi:10.1029/2002JA009343.  
 Usoskin, I. G., S. K. Solanki, M. Schüssler, K. Mursula, and K. Alanko (2003), Millennium-scale sunspot number reconstruction: Evidence for an unusually active Sun since the 1940s, *Phys. Rev. Lett.*, **91**, 211101.

- Usoskin, I. G., N. Marsh, G. A. Kovaltsov, K. Mursula, and O. G. Gladysheva (2004a), Latitudinal dependence of low cloud amount on cosmic ray induced ionization, *Geophys. Res. Lett.*, *31*, L16109, doi:10.1029/2004GL019507.
- Usoskin, I. G., O. G. Gladysheva, and G. A. Kovaltsov (2004b), Cosmic ray induced ionization in the atmosphere: Spatial and temporal changes, *J. Atmos. Sol. Terr. Phys.*, *66*, 1791.
- Wang, J. Z., et al. (2002), Measurement of cosmic-ray hydrogen and helium and their isotopic composition with the BESS experiment, *Astrophys. J.*, *564*, 244.
- Webber, W. R., and P. R. Higbie (2003), Production of cosmogenic Be nuclei in the Earth's atmosphere by cosmic rays: Its dependence on solar modulation and the interstellar cosmic ray spectrum, *J. Geophys. Res.*, *108*(A9), 1355, doi:10.1029/2003JA009863.
- Webber, W. R., et al. (1991), A measurement of the cosmic-ray H-2 and He-3 spectra and H-2/He-4 and He-3/He-4 ratios in 1989, *Astrophys. J.*, *380*, 230.
- 
- K. Alanko-Huotari and K. Mursula, Department of Physical Sciences, University of Oulu, P.O. Box 3000, FIN-90014 Oulu, Finland.
- G. A. Kovaltsov, Ioffe Physical-Technical Institute, Politekhnicheskaya 26, RU-194021 St. Petersburg, Russia.
- I. G. Usoskin, Sodankylä Geophysical Observatory (Oulu Unit), University of Oulu, P.O. Box 3000, FIN-90014 Oulu, Finland. (ilya.usoskin@oulu.fi)